

flooded environments. During the mining process at the working face, residual coal often falls into waterlogged areas. After being soaked in water and subsequently air-dried, it transforms into immersed coal.^{5,6} Water immersion causes significant changes in the physical and chemical properties of coal, especially when compared to raw coal.⁷ As coal seams are mined, the water that accumulates in the goaf gradually drains away, leading to the formation of additional fractures in the overlying rock layers. This process creates intricate air leakage pathways, which, in turn, expand the contact area between the residual coal and oxygen. Due to the increased air leakage intensity, water-immersed coal bodies experience further dehydration and drying. During the mining or unsealing of working faces, these coal bodies become more susceptible to oxidation, which, in turn, elevates their risk of spontaneous combustion.

At present, many scholars have carried out a large number of experimental studies on the influence of water immersion on the oxidation stage of coal, mainly focusing on activation energy, characteristic temperature, heat absorption, discharge, etc., which provides important theoretical and practical support for solving the problem of coal spontaneous ignition after the drainage of water immersion gob in coal mines. Bu et al.⁸ employed a programmed temperature oxidation apparatus to examine the changes in kinetic parameters for both raw and water-immersed coal at various oxidation stages under different oxygen concentrations. Their observations revealed that during the third oxidation stage, the heat release rate of the water-immersed coal samples was lower compared to that of the untreated coal. Zhang et al.⁹ divides the low-temperature oxidation process of coal into three stages according to the production rate of CO and CO₂. Through gray correlation analysis, it is found that soaking water has the most significant effect on the accelerated oxidation of coal. Through the study of thermogravimetric analyzer, Zhang et al.¹⁰ found that water immersion can inhibit the water evaporation stage of coal and promote the water immersion in the oxygenation stage and the combustion weight loss stage. Deng et al.¹¹ found that under the same heating rate, water-soaked air-dried coal has less heat absorption stage, and its peak heat absorption temperature is lower than that of raw coal. Liu et al.¹² divided the variation curve of minimum floating coal thickness (Hmin) with temperature into three stages and found that the Hmin sequence of stage II and stage III was the same as that of stage I, indicating that at the same temperature, the thermal enrichment of water-impregnated coal and oxidized coal was more obvious, and coal spontaneous combustion was more likely to occur. Huang et al.¹³ used thermogravimetric analysis to divide the quality change of water-impregnated coal in the process of temperature-programmed oxidation into three stages. Zhang et al.¹⁴ found that the oxidation characteristic temperature points on TG and DSC curves and the activation energy *E* of TG at the second and third stages were significantly lower than that of the immersed coal at room temperature.

The evolution of coal's spontaneous combustion characteristics is essentially due to the change of its internal chemical structure. Therefore, it is very important to explore the evolution law of coal microstructure after water immersion to reveal the mechanism of coal spontaneous combustion and its control strategies. Zhong et al.¹⁵ compared and analyzed the difference of the initial functional group structure and the evolution rule of the two coal samples in the oxidation process by measuring the three-dimensional in situ Fourier transform infrared spectrum of

the spontaneous combustion water-immersed coal and raw coal in the process of low-temperature oxidation. Guo et al.¹⁶ used Fourier transform infrared (FTIR) spectroscopy to analyze the chemical structure of raw coal and soaking coal. Lu et al.¹⁷ used infrared spectrum to qualitatively analyze the distribution and change of functional groups before and after coal immersion in water. Huang et al.¹⁸ conducted in situ infrared spectroscopy experiments to investigate the changes in functional groups in coal both before and after water immersion, while also assessing the effect of temperature on these transformations. Their results revealed that water immersion reduced the temperatures at which internal aliphatic hydrocarbons and oxygen-containing functional groups started reacting with oxygen to form coal-oxygen complexes. Zhai et al.¹⁹ found that, compared to untreated coal, water-immersed coal samples exhibited longer side chains and a greater degree of branching in the aliphatic side chains. This indicates an increased tendency for spontaneous combustion.

In summary, current research mainly focuses on the impact of water immersion on the overall oxidation stages of coal, while there is limited study of the spontaneous combustion characteristics and specific evolution patterns of key functional groups during the low-temperature oxidation stages of coal. In China's bituminous coal mining regions, spontaneous combustion incidents involving water-immersed coal are common, with long-flame coal and fat coal representing a significant proportion of the bituminous coal involved. Building on this, this study selected long-flame coal and fat coal as the research subjects. This study employs scanning electron microscopy, low-temperature nitrogen adsorption, programmed temperature rise-gas chromatography, and in situ Fourier transform infrared spectroscopy to examine how the microstructural properties of long-flame coal and fat coal are altered under different water immersion conditions. In addition, we analyzed the rates of gaseous product formation throughout the heating and oxidation process, determined the apparent activation energy, and investigated the variations in the active functional groups at each stage of the reaction. Moreover, Pearson correlation analysis was employed to pinpoint the crucial functional groups in bituminous coal at different stages of low-temperature oxidation. The results of this study enhance our understanding of how water immersion influences the spontaneous combustion characteristics of bituminous coal, offering a theoretical foundation for the prevention and control of spontaneous combustion under similar conditions.

2. COAL SAMPLE PREPARATION AND EXPERIMENTAL METHODS

2.1. Experimental Coal Sample Preparation. This research concentrated on samples of long-flame coal and fat coal sourced from the Datong mining area in Shanxi Province. First, freshly collected coal samples were obtained from the active mining face of the coal seam, sealed in containers, and then transported to the laboratory for subsequent analysis. The oxidized layer on the surface of the samples was meticulously stripped away, after which the coal was crushed by using a jaw crusher. The resulting material was then screened to isolate coal samples with mesh sizes ranging from 60 to 80. By mixing 60 g coal samples with different amounts of water by an electric mixer, 6 groups of coal samples with a mass ratio of water and long-flame coal and fat coal are 1:2, 1:1, and 2:1, respectively. These were named C(1:2), C(1:1), C(2:1), F(1:2), F(1:1), and F(2:1), respectively.²⁰ The long-flame coal and fat coal without a

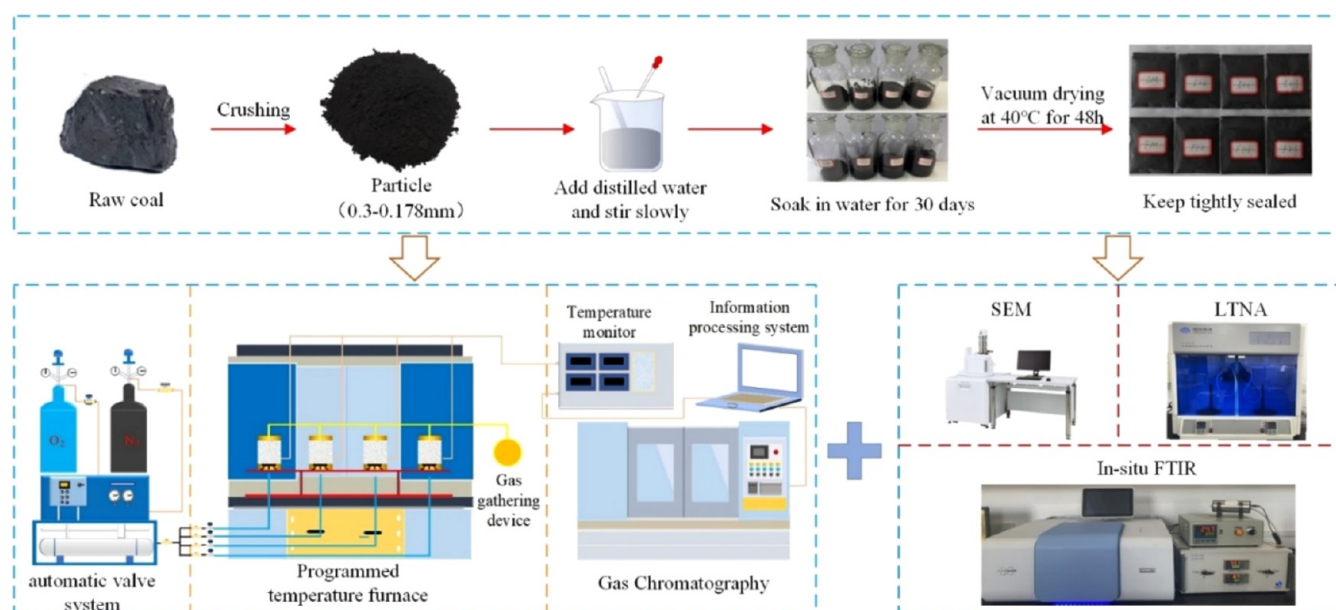


Figure 1. Schematic of coal sample preparation and experimental procedures.

Table 1. Proximate Analysis and Elemental Coal

samples	proximate analysis (%)				ultimate analysis (%)			
	M_{ad}	A_{ad}	V_{ad}	FC_{ad}	C_{daf}	H_{daf}	O_{daf}	N_{daf}
CM	4.51	3.28	32.37	59.84	74.35	3.67	1.81	20.17
FM	4.26	3.82	27.56	64.36	77.72	3.11	1.38	17.79

water immersion treatment were named CM and FM, respectively. The prepared samples were stored in a cool environment for 30 days, after which they were vacuum-dried at 40 °C for 48 h. Ultimately, both the untreated coal samples and the vacuum-dried, water-immersed coal samples were sealed and stored for future analysis. The process flow for preparing the coal samples and conducting the experiments is illustrated in Figure 1. Moreover, Table 1 provides the results of the industrial and elemental analyses conducted on both long-flame coal and fat coal.

2.2. Controlled Temperature Increase Experiment.

The programmed temperature increase experiment employed a gas chromatography device independently developed by North China University of Science and Technology. Its main components include a gas generator, a programmed temperature furnace, a gas chromatograph, and an information processing system. Experimental Steps: Weigh 50 g of raw coal and water-immersed coal samples, place them into the heat transfer coal sample tank, cover evenly with a 2–3 mm thick asbestos layer to prevent coal dust from clogging the pipeline; connect the gas circuit and check the airtightness of the device, set the flow meter parameter to 100 mL·min⁻¹. Heating Program: Increase the temperature from room temperature to 30 °C within 10 min,²¹ maintain at a constant temperature of 30 °C for 20 min, then increase at a rate of 2 °C·min⁻¹ until it reaches 220 °C. Before 100 °C, collect gas samples every 10 °C interval; after 100 °C, collect gas samples at every 20 °C interval. The collected gases are then analyzed for their components using a gas chromatograph. Repeat the above experimental steps to obtain the gas composition and concentration generated by long-flame coal and fat coal at various temperature stages under different water immersion conditions.

2.3. Scanning Electron Microscopy and Low-Temperature Nitrogen Adsorption Experiment.

A Zeiss GeminiSEM 360 scanning electron microscope (SEM) was employed to examine the pores and fractures in both long-flame coal and fat coal under various water immersion conditions. The scanning parameters were set as follows: acceleration voltage of 3.00 kV, resolution of 1.0 μm, and operation in high vacuum mode. In order to enhance the conductivity of the coal samples and protect the instrument, a thin layer of gold was applied to the samples prior to the experiment.

The experiment was conducted using a JW-BK112 static nitrogen adsorption instrument produced by Beijing Jingwei Gao Bo. The experimental steps include: Taking 2 g of raw coal and water-treated coal samples, placing them separately in physical adsorption containers, ensuring that the samples are dry before operation to avoid interference from external moisture; accurately weighing the sample tube to m_0 , then connecting the sample tube to the nitrogen adsorption instrument for degassing treatment. The degassing process involves heating in a vacuum environment at a rate of 5 °C/min to 150 °C and maintaining for 1 h to remove volatile impurities and adsorbed moisture from the sample; after degassing is completed, slowly cool the sample tube to room temperature and equilibrate under nitrogen protection to ensure stable sample temperature and prevent readsorption of moisture; place the degassed sample tube into the adsorption instrument, start the low-temperature nitrogen adsorption experiment, record the nitrogen adsorption and desorption curves, and maintain stability through a constant temperature device; at the end of the experiment, automatically collect and generate the nitrogen adsorption isotherm. Finally, the total weight of the sample tube and its contents after the

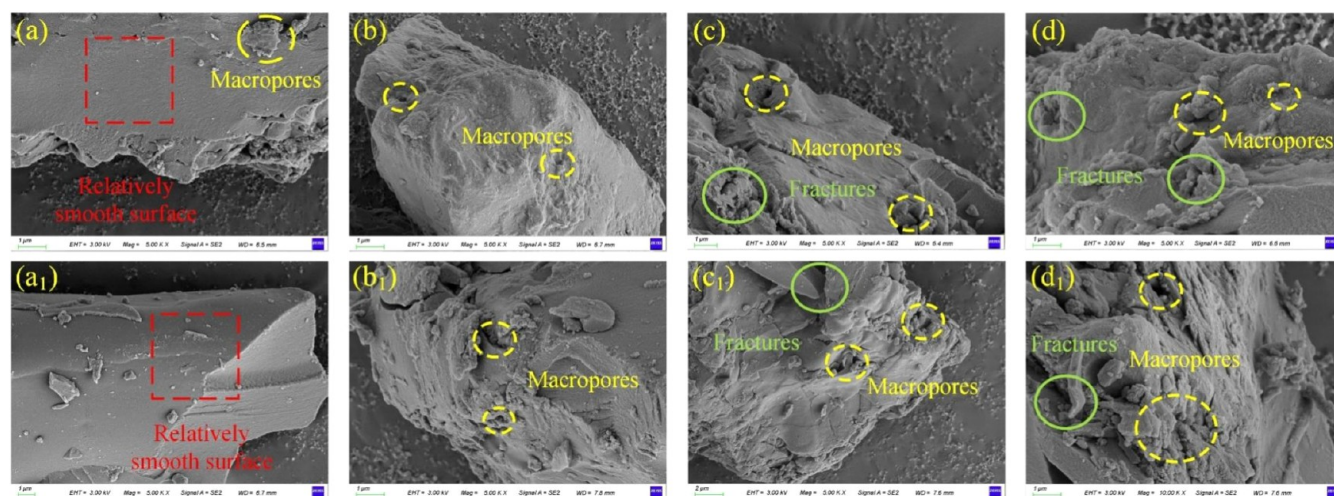


Figure 2. SEM micrographs of coal samples: (a) CM; (a₁) FM; (b) C1:2; (b₁) F1:2; (c) C1:1; (c₁) C1:1; (d) C2:1; (d₁) C2:1.

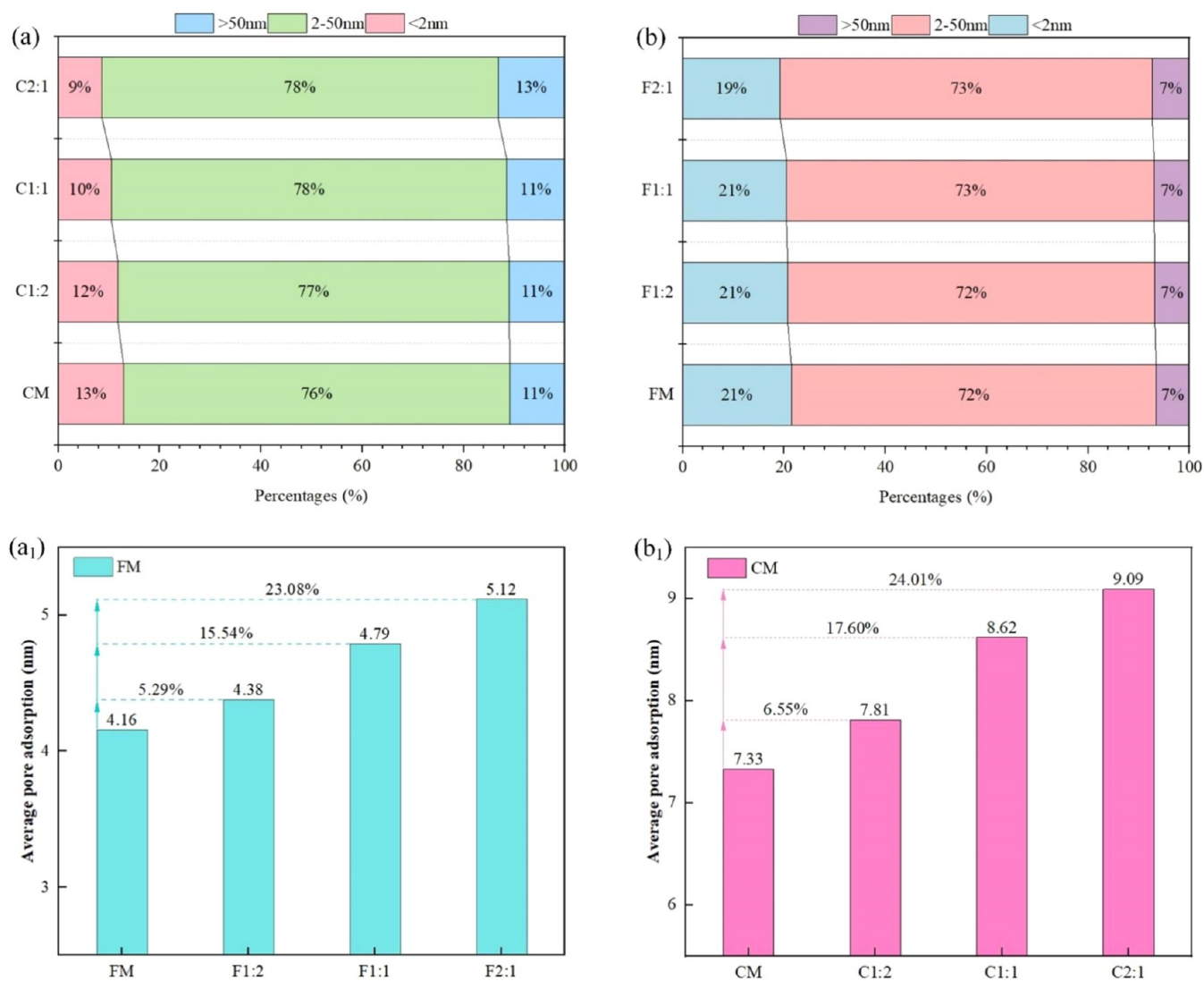


Figure 3. Diagrams of average pore diameter and pore structure distribution ratio for long-flame coal and fat coal: (a, a₁) long-flame coal; (b, b₁) fat coal.

experiment were weighed as m_1 , and the actual adsorption amount of the sample was determined by calculating the difference between m_0 and m_1 .

2.4. In Situ FTIR Experiment. The infrared spectrum analysis was conducted by using a Fourier transform infrared spectrometer (Bruker VERTEX 70), which was fitted with a

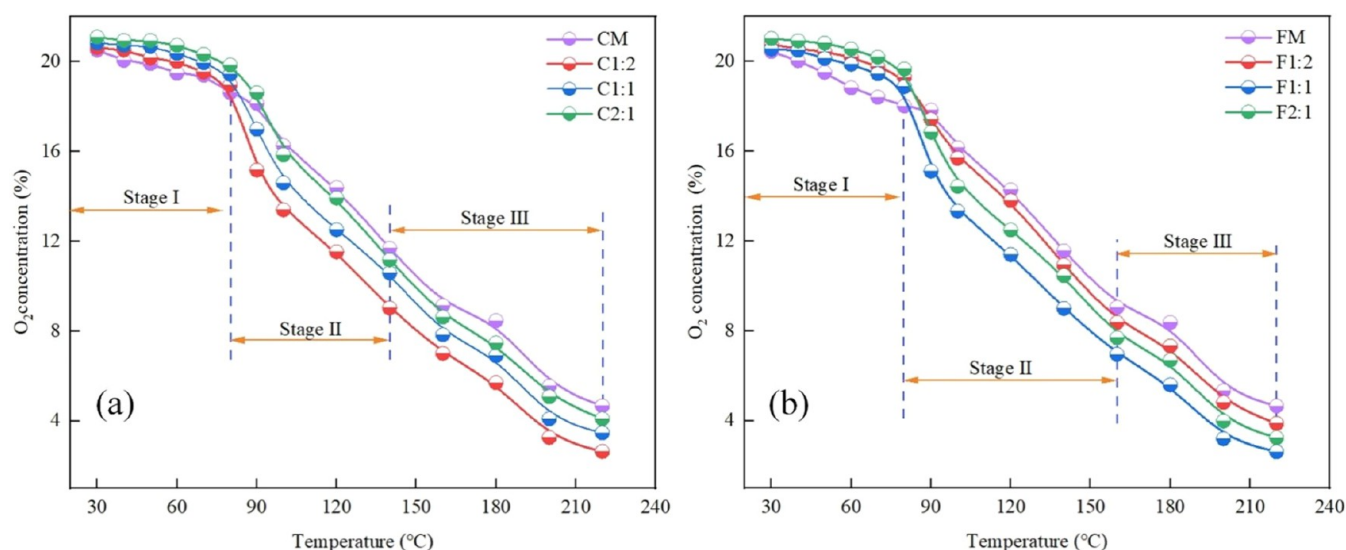


Figure 4. O₂ concentration curve of long-flame coal and fat coal under different water leaching conditions: (a) long-flame coal; (b) fat coal.

PiKE in situ reaction cell. The measurement wavelength range was 700–4000 cm^{−1}, and the scanning rate was 64 times per second. During the experiment, the sample and potassium bromide were ground and mixed in a mass ratio of 1:100. The uniformly mixed sample was placed in the reaction cell, and the heating program was set to heat from 40 to 240 °C at a rate of 10 °C/min. Infrared spectroscopy scans of the coal samples were performed every 20 °C (before the start of the experiment, KBr was scanned as a background).

2.5. Pearson's Correlation Analysis Method. The Pearson correlation coefficient,²² alternatively referred to as the Pearson product-moment correlation coefficient, is a statistical measure used to evaluate the strength and direction of the relationship between two variables, *X* and *Y*. It is calculated by dividing the covariance of the two variables by the product of their individual standard deviations. The general formula for determining the correlation coefficient (*R*) is presented below:

$$R = \frac{\text{Cov}(X, Y)}{D(X)D(Y)} = \frac{E[(X - \mu_X)(Y - \mu_Y)]}{D(X)D(Y)} \quad (1)$$

The Pearson correlation coefficient can be expressed as the ratio of the covariance and standard deviations of the sample as follows:

$$R = \frac{\sum_{i=1}^n (X_i - \bar{X})(Y_i - \bar{Y})}{\sqrt{\sum_{i=1}^n (X_i - \bar{X})^2} \sqrt{\sum_{i=1}^n (Y_i - \bar{Y})^2}} \quad (2)$$

where *X*, *Y*: two variables, representing two different features used to calculate correlation; *R*: Pearson correlation coefficient; *n*: number of samples.

When the Pearson correlation coefficient *R* is 0, it indicates no correlation between the variables. When *R* falls between 0 and ±0.3, this suggests a weak positive or negative correlation. If *R* lies between ±0.3 and ±0.5, it indicates a low-level positive or negative correlation. When *R* is between ±0.5 and ±0.8, it reflects a significant positive or negative correlation. Finally, when *R* is between ±0.8 and ±1.0, it indicates a high level of positive or negative correlation between the variables.

3. RESULTS AND DISCUSSION

3.1. Surface Microstructure and Pore Distribution of Coal Samples before and after Water Immersion. This study explores how water immersion affects the surface structure and pore distribution characteristics of long-flame coal and fat coal, with particular emphasis on the microstructural level. The analysis is performed by using SEM and LTNA techniques. This forms a foundational basis for examining the stages of spontaneous combustion behavior and investigating the key functional groups involved. Figure 2 presents the SEM images of long-flame coal and fat coal under various water immersion conditions.

It can be seen from Figure 2a–d, a₁–d₁ that the surfaces of long-flame coal and fat coal without water immersion treatment are relatively smooth, with fewer large pores and cracks. Following water immersion, the coal exhibits an increase in the number of pore cracks. Additionally, with the increase in water immersion volume, the coal's pore structure becomes increasingly developed. When the water-to-coal mass ratio of long-flame coal and fat coal is 1:2, a few cracks emerge on the surface of both coals, resulting in a slightly rough texture. As the water-to-coal mass ratio increases to 1:1, the number of pore cracks in the coal rises, with the pores becoming interconnected to form intricate coal-oxygen contact pathways. This progressively leads to a more porous coal structure. When the water-to-coal mass ratio reaches 2:1, there is a marked increase in both the number of cracks and large pores in the coal sample with enhanced connectivity. This creates additional pathways for oxygen diffusion and release of volatile substances.

The effect of water immersion on the pore structure of bituminous coal was quantitatively assessed by using LTNA. The aperture distribution and average pore diameter of both long-flame coal and fat coal, under different water immersion conditions, are shown in Figure 3a,b, a₁, b₁, respectively.

As shown in Figure 3a,b, under water immersion conditions, the proportion of micropores in both long-flame coal and fat coal gradually decreases. Specifically, it drops from 12.85 and 21.87% before water immersion to 8.65 and 19.64%, respectively. At the same time, the proportion of mesopores increases, with the most notable rise observed in long-flame coal, where it increases from 76.31 to 78.16%. This occurs because water immersion causes

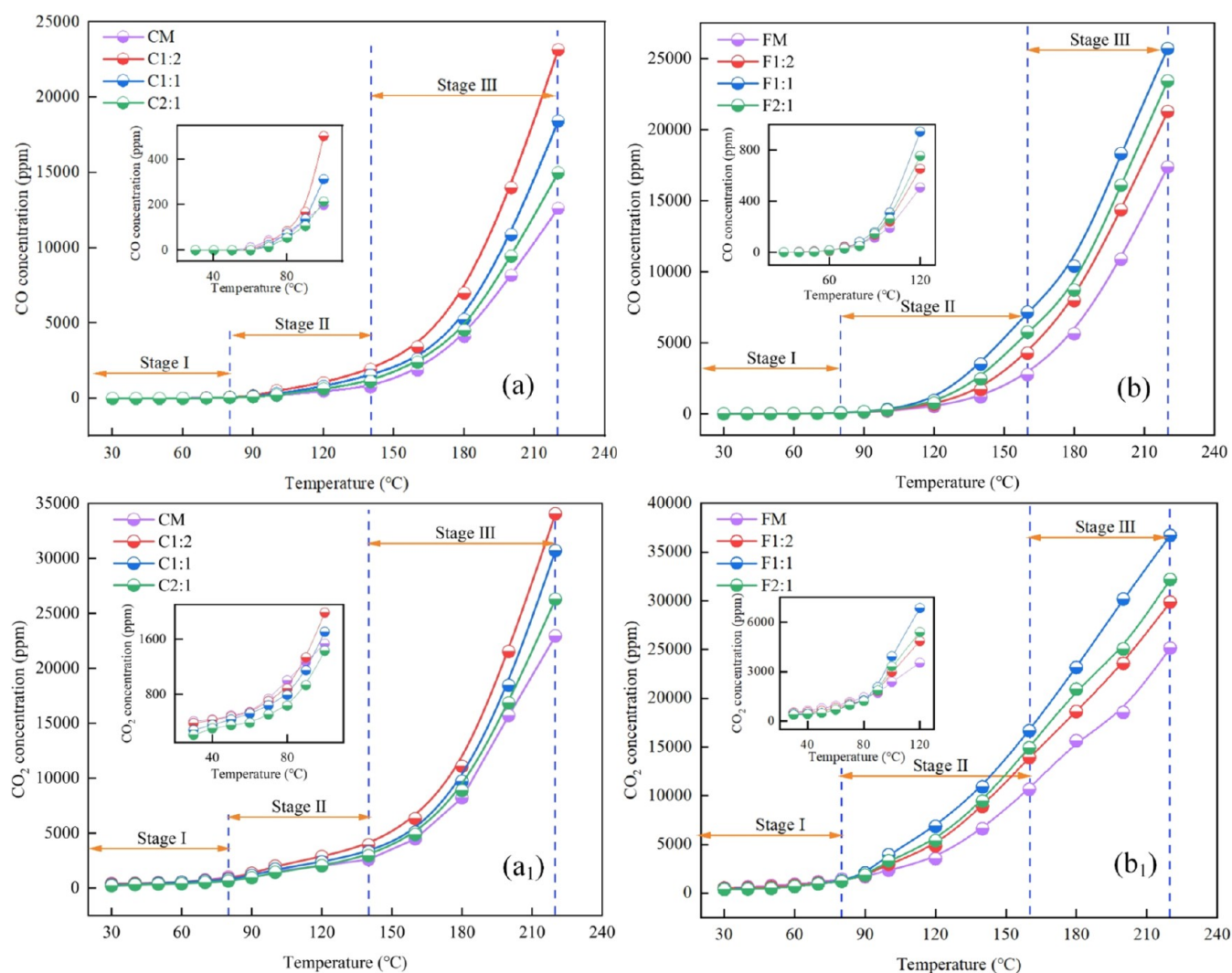


Figure 5. Change curves of CO and CO₂ concentrations of long-flame coal and fat coal under different leaching water quantities: (a, a₁) long-flame coal; (b, b₁) fat coal.

soluble minerals and organic matter within the micropores of coal to dissolve. Through bridging effects, these processes lead to the formation of mesopores.²³ In addition, water immersion results in an increase in the proportion of large pores in two types of bituminous coal with different metamorphic degrees, in which the proportion of long-flame coal increases from 10.84 to 13.19% and the proportion of fat coal increases from 6.72 to 7.52%. This observation is consistent with the changes in the surface morphology seen under SEM.

As seen in Figure 3a₁,b₁, the average pore diameters of both long-flame coal and fat coal gradually increase as the duration of water immersion increases. When the water-to-coal mass ratios are 1:2, 1:1, and 2:1, the average pore diameters of long-flame coal are 4.38, 4.79, and 5.12 nm, respectively, while for fat coal, the average pore diameters are 7.81, 8.62, and 9.09 nm, respectively. After water immersion, the average pore diameter of long-flame coal increased by 6.55, 17.60, and 24.01%, while that of fat coal increased by 5.29, 15.54, and 23.08%. Water immersion has a more pronounced effect on long-flame coal, resulting in a greater increase in the average pore diameter compared to fat coal. The observed difference can be attributed to the lower metamorphic rank of long-flame coal, which has a more developed pore structure. This characteristic facilitates the

transformation of micropores into mesopores and macropores more readily.²⁴ Additionally, long-flame coal contains a higher content of soluble minerals and organic matter internally. The dissolution process is more pronounced during water immersion, further promoting expansion of the pore diameters.

3.2. Analysis of Programmed Temperature Rise-Gas Chromatography Experiment Results. **3.2.1. O₂ Concentration Consumption Analysis.** The variation in the concentration of the O₂ with temperature during the programmed temperature rise process for both long-flame coal and fat coal under different water immersion conditions is shown in Figure 4.

As shown in Figure 4a,b, under various water immersion conditions, the oxygen concentrations in both long-flame coal and fat coal gradually decrease as the temperature increases. However, the rate of decline follows a pattern of being initially slow, then rapid, and finally becoming more intense as the temperature rises. Based on the oxygen consumption rate, the oxidation of coal samples induced by temperature can be divided into three stages: slow oxidation, rapid oxidation, and intense oxidation.^{25,26} During the slow oxidation phase (Stage I), which occurs between 30 and 80 °C, the oxygen concentration in both long-flame coal and fat coal decreases gradually as the temperature increases. Among these, the oxygen concentration

in CM and FM experiences the most significant decline, with their oxygen consumption rates notably higher than those of the water-immersed coal samples. The oxygen concentration decreases from initial values of 20.52 and 20.44% to 18.61 and 18.02%, respectively. This is mainly attributed to water immersion, which raises the moisture content within the coal's pores, consequently slowing the oxidation process. When heated, the evaporation of water absorbs some of the heat generated during the low-temperature oxidation of bituminous coal, thereby reducing the rate of the oxidation reaction.²⁷

Due to the lower metamorphic degree of long-flame coal, its pore structure is more developed, with a relatively higher proportion of macro- and mesopores. This structure facilitates a more rapid oxidation reaction.²⁸ As a result, the rapid oxidation phase of long-flame coal concludes earlier than that of the fat coal. During the rapid oxidation stage (Stage II), the temperature range for long-flame coal is between 80 and 140 °C, whereas for fat coal, it extends from 80 to 160 °C. The oxygen concentration decreases rapidly as the temperature increases during this stage. Among the samples, C1:2 and F1:1 exhibit the highest oxygen consumption, reaching 9.94 and 10.93%, respectively. These values are 1.43 and 1.21 times higher than that of raw coal. This phenomenon may be explained by the fact that as the temperature increases, the moisture in the pores gradually evaporates, which enhances the oxygen flow rate within the coal and thus accelerates the oxidation process. As a result, with the evaporation of moisture, the coal shifts from physical and chemical adsorption to more vigorous chemical reactions, thereby accelerating the oxidation process. During the intense oxidation stage (Stage III), the temperature range for long-flame coal is between 140 and 220 °C, whereas for fat coal, it extends from 160 to 220 °C. During this stage, as the temperature increases, the oxygen concentration drops significantly. The oxygen consumption of C1:2 and F1:1 coal samples is the highest, which are 4.77 and 4.34%, respectively. By this point, all moisture in the coal has evaporated, and the porosity of the coal increases further, which promotes a faster oxidation process. As the contact area between coal and oxygen increases significantly, the reaction becomes more vigorous. This enhanced interaction accelerates the oxidation process, reaching a maximum intensity.

3.2.2. CO and CO₂ Production Analysis. Figure 5 illustrates the production of CO and CO₂ from long-flame coal and fat coal under varying water immersion conditions during the programmed temperature increase process.

As seen in Figure 5a,a₁,b,b₁, under different water immersion conditions, the generation rates of CO and CO₂ in both long-flame coal and fat coal exhibit a trend of initially slow increase, followed by a rapid rise and finally a sharp increase as the temperature rises. Additionally, the generation patterns of CO and CO₂ are consistent with oxygen consumption, exhibiting similar segmented characteristics and corresponding temperature ranges. In the slow oxidation stage, both long-flame coal and fat coal exhibit low generation rates of CO and CO₂, which gradually rise as the temperature increases. Notably, CO₂ is consistently produced throughout the entire heating oxidation process. However, there is a difference in the initial CO generation temperature. For the non-water-immersed long-flame coal and fat coal, the initial CO generation temperatures are 60 and 70 °C, respectively, with production amounts of 11.90 and 8.07 ppm.

During the rapid oxidation stage, as the coal temperature further increases, chemical reactions accelerate, leading to a

rapid rise in the level of CO and CO₂ gas production. Experimental results indicate that for CM coal samples, the generation of CO and CO₂ reached peak values of 753 and 2554 ppm, respectively, at 140 °C. For FM coal samples, the generation of CO and CO₂ reached peak values of 2755 and 10,661 ppm, respectively, at 160 °C. This difference is primarily due to the lower degree of metamorphism in long-flame coal, which makes it more susceptible to oxidative decomposition under the same temperature conditions. As a result, the reaction extent is higher, leading to greater CO production.²⁹ In the intense oxidation stage, the production of CO and CO₂ increases sharply with temperature and the generation rate escalates dramatically. The production of CO and CO₂ from long-flame coal and fat coal does not show a linear increase with the amount of water immersion. At 220 °C, the CO production from the C1:2 and F1:1 coal samples is the highest, reaching 23,157 and 25,699 ppm, respectively. This represents an increase of 1.83 and 1.48 times compared to raw coal. The production of CO reflects the intensity of the coal oxidation reactions. Therefore, when the mass ratio of water to long-flame coal is 1:2 and the mass ratio of water to fat coal is 1:1, the spontaneous combustion tendency is the highest.

3.2.3. Analysis of Kinetic Parameters. Building on the results from the programmed temperature rise experiments, the activation energy for both long-flame coal and fat coal was calculated to further investigate how water immersion influences the spontaneous combustion properties of bituminous coal. This method offers a comprehensive, quantitative analysis of how water immersion affects the coal's behavior during various stages of oxidation. The activation energy is determined by assessing the oxygen consumption of the coal samples during the programmed temperature increase. This enables a quantitative evaluation of the energy needed for oxidation reactions in various stages of coal heating.

The formula used to calculate oxygen consumption is provided below:³⁰

$$v_{O_2}^0(T) = -j\rho_g c_{O_2}^2 A_0 \exp\left(-\frac{E_a}{RT}\right) \quad (3)$$

To simplify the calculation process, the difference between the inlet oxygen concentration and the outlet oxygen concentration during coal oxidation can be considered as oxygen consumption. This difference reflects the amount of oxygen consumed by the coal during the oxidation process at each temperature stage:

$$-v_{O_2}^0(T)V = m(c_{O_2}^2 - c_{O_2}^1) \quad (4)$$

By combination of eqs 3 and 4, the following expression can be obtained:

$$\ln \frac{c_{O_2}^1 - c_{O_2}^2}{c_{O_2}^2} = -\frac{E_a}{RT} + \ln\left(\frac{V}{m} \rho_g A_0\right) \quad (5)$$

where ρ_g is the gas density, kg/m³; E_a represents the apparent activation energy, J/mol; R is the gas constant, 8.314 J/(K·mol); S^{-1} is the pre-exponential factor; A_0 is the porosity; $c_{O_2}^1$ denotes the oxygen concentration at the inlet, %; $c_{O_2}^2$ represents the oxygen concentration at the outlet, %; and j is the porosity.

Because the difference between the inlet oxygen concentration and the outlet oxygen concentration in Stages I is smaller, the accuracy of $\ln \frac{c_{O_2}^1 - c_{O_2}^2}{c_{O_2}^2}$ is relatively low. Therefore, Stages II

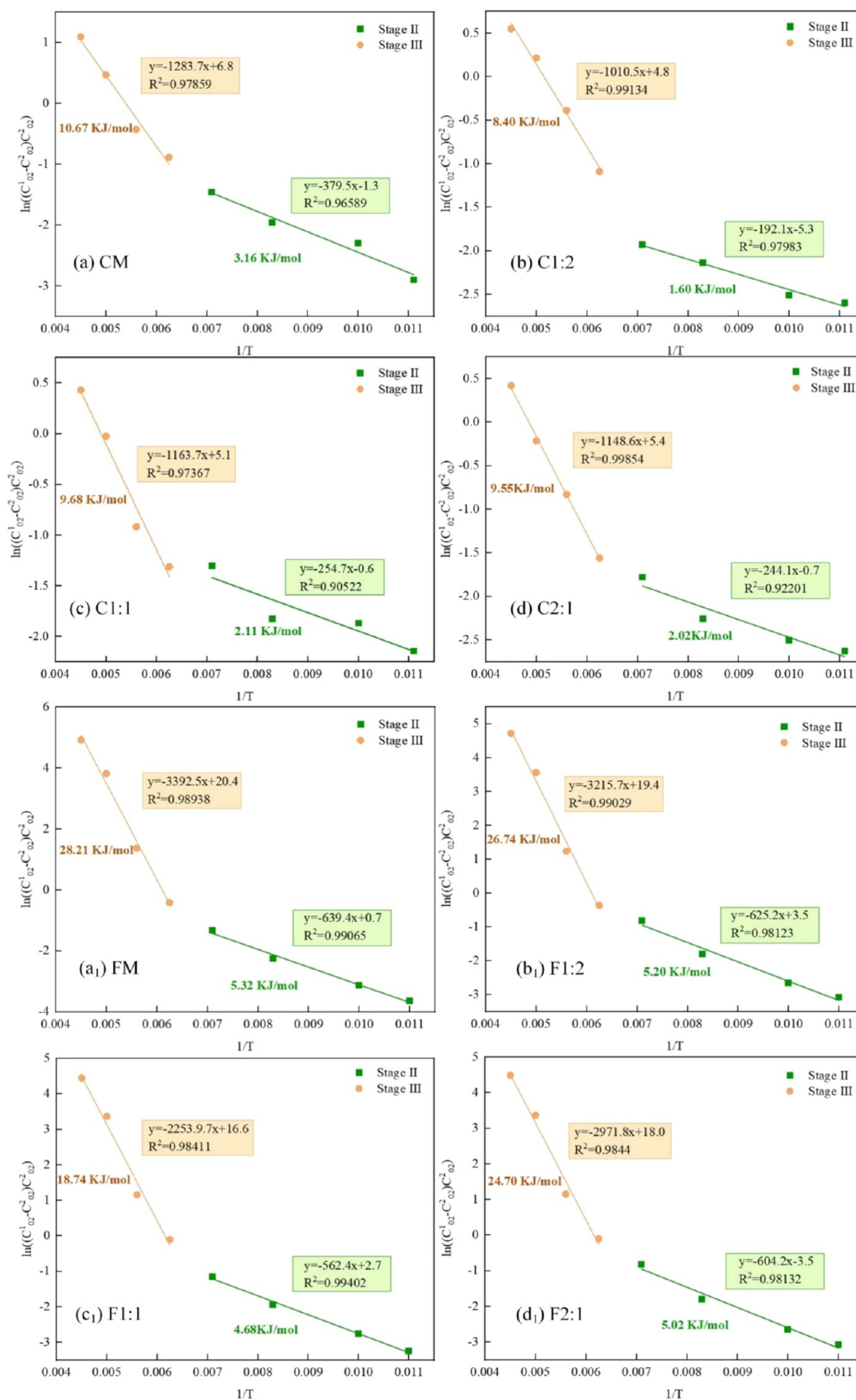


Figure 6. Comparison of apparent activation energies of long-flame coal (a–d) and fat coal (a₁–d₁) at different temperature oxidation stages under different leaching water conditions.

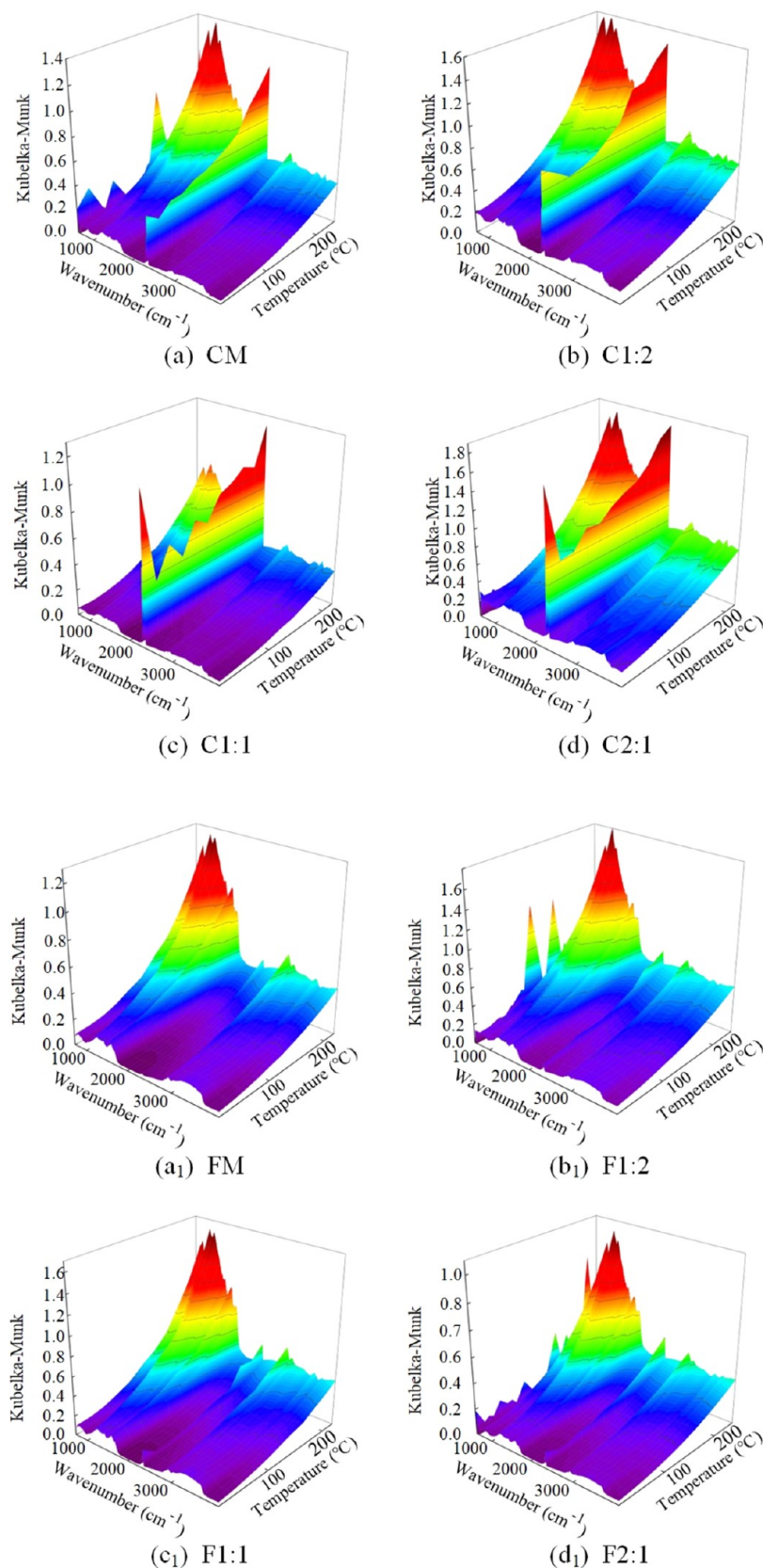


Figure 7. In situ infrared spectra of long-flame coal (a–d) and fat coal (a₁–d₁) under different water leaching conditions.

and III are selected for the analysis of the activation energy changes.

The $\ln \frac{c_{O_2}^1 - c_{O_2}^2}{c_{O_2}^2}$ is linearly related to $\frac{1}{T}$. By fitting the experimental data into eq 5, the activation energies for both

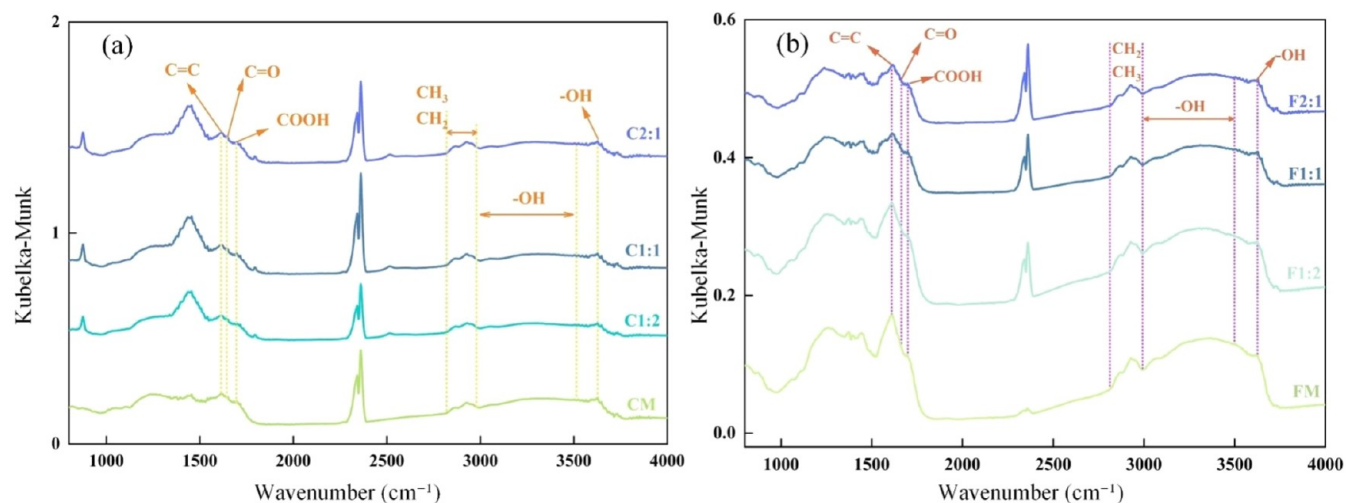


Figure 8. Results of Fourier transform infrared (FTIR) spectroscopy analysis for coal samples, both before and after water immersion treatment: (a) long-flame coal; (b) fat coal.

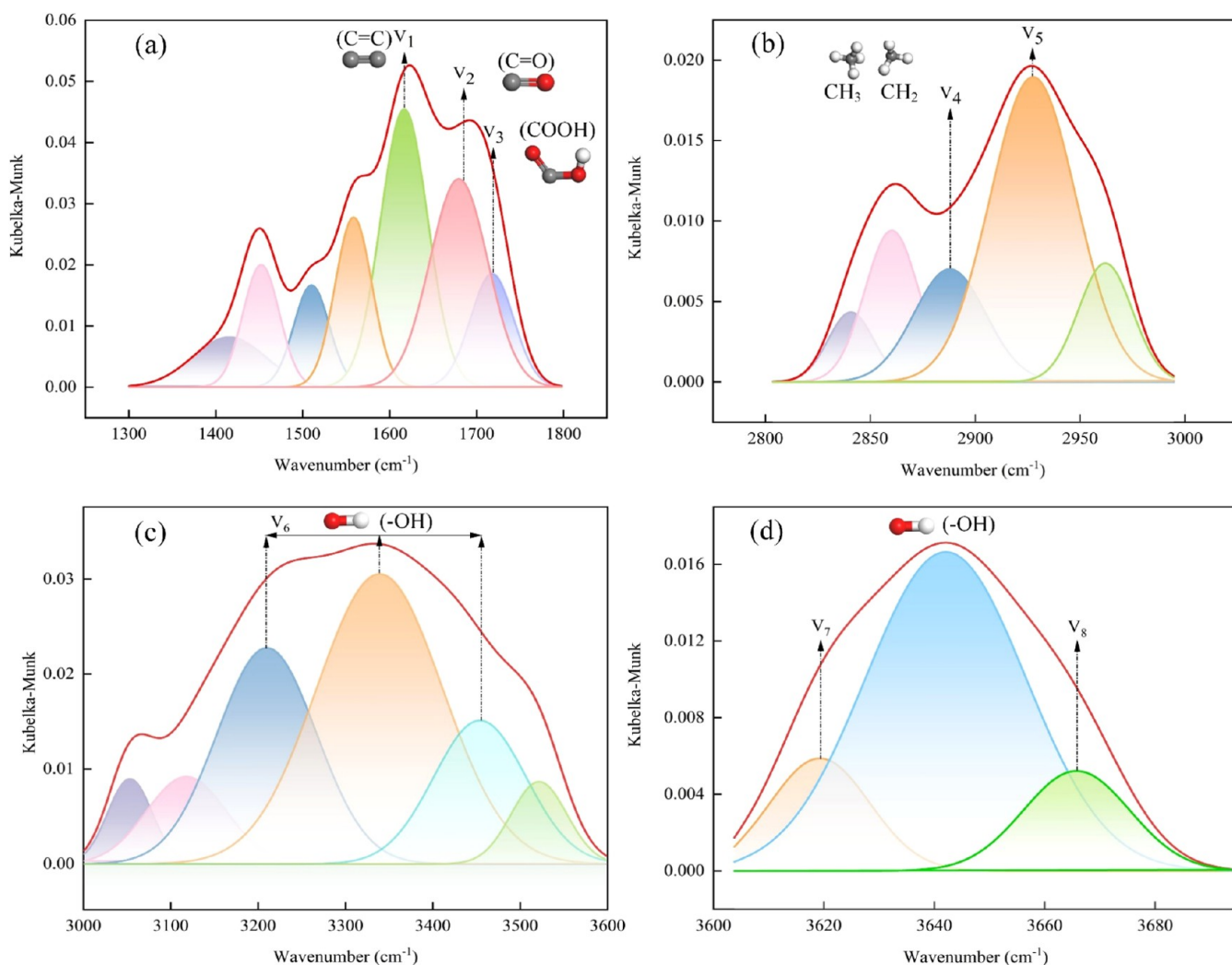


Figure 9. FTIR peak fitting diagram of long-flame coal in different wavenumber bands.

long-flame coal and fat coal during Stages II and III, under various water immersion conditions, can be determined. The fitting curves and activation energy E_a are shown in Figure 6.

As shown in Figure 6, the change of leaching water has little influence on the activation energy of long-flame coal and fat coal during stage II of heating oxidation. The activation energies for CM, C1:2, C1:1, C2:1 and FM, F1:2, F1:1, and F2:1 are 3.16,

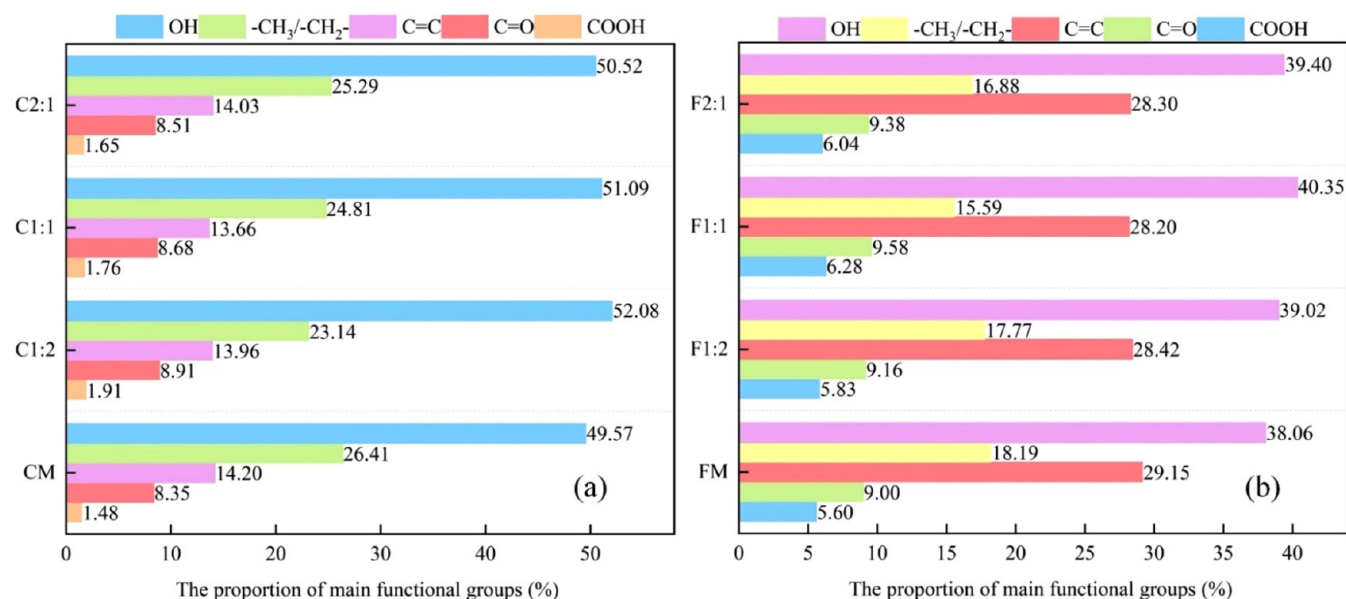


Figure 10. Percentage of main active functional groups in experimental coal samples at 40 °C: (a) long-flame coal; (b) fat coal.

1.60, 2.02, and 2.11 kJ/mol and 5.32, 5.20, 4.68, and 5.02 kJ/mol, respectively. This is attributed to the fact that Stage II primarily involves the evaporation of internal moisture and the thermal breakdown of macromolecules in the coal, during which oxygen plays a relatively minor role in the reaction.³¹ During Stage III, the activation energy of the coal samples decreases due to water immersion. With an increase in water immersion, the activation energy first rises and then falls. This indicates a complex relationship between the water content and the coal's oxidation characteristics at elevated temperatures. The activation energies for long-flame coal and fat coal, when not subjected to water immersion, are 10.67 and 28.21 kJ/mol, respectively. Both values are greater than the activation energies observed for the coal samples that underwent water immersion, suggesting that water immersion helps to reduce the activation energy, thereby promoting the oxidation process and increasing the likelihood of spontaneous combustion. Compared to raw coal, the activation energy of C1:2, C1:1, C2:1 and F1:2, F1:1, F2:1 has decreased by 21.2, 10.5, 9.27% and 5.21, 33.5, 12.4%, respectively. This suggests that even a small amount of water immersion enhances the self-ignition tendency of bituminous coal by reducing the activation energy, thus facilitating the oxidation process. However, excessive water immersion may inhibit the oxidation process by saturating the coal, which reduces the available surface area for the reaction and, in turn, decreases its reactivity.

3.3. In Situ Infrared Analysis. The variation in functional groups was investigated by analyzing the FTIR spectra of both raw coal and coal samples subjected to different water immersion conditions. This analysis provided a clearer understanding of how water immersion affects the functional groups in coal, shedding light on the mechanisms by which it alters the chemical structure and reactivity of the coal. Figure 7 displays the in situ infrared spectra of long-flame coal and fat coal subjected to different water immersion conditions.

3.3.1. Analysis of the Infrared Spectral Characteristics of Long-Flame Coal and Fat Coal at Ambient Temperature. By examination of how water immersion affects the functional groups in long-flame coal and fat coal at room temperature, the inherent chemical properties of the coal can be uncovered

without the need for external thermal activation. This analysis offers valuable data for understanding how functional groups evolve during the heating process, shedding light on the chemical transformations that may take place as coal undergoes various thermal conditions. At 40 °C, the infrared spectra of long-flame coal and fat coal with water-to-coal mass ratios of 1:2, 1:1, and 2:1 are shown in Figure 8.

As shown in Figure 8a,b, a noticeable increase in the intensity of characteristic peaks for hydroxyl groups (–OH) and oxygen-containing functional groups (such as carbonyl C=O and carboxyl COOH) is observed in both long-flame coal and fat coal after water immersion compared to the raw coal samples. This indicates that water immersion promotes the formation of these polar groups. However, the absorption peak strength of aliphatic hydrocarbons (–CH₃/–CH₂) decreased only slightly, while that of aromatic hydrocarbons (C=C) changed more slowly, indicating that the structure of aromatic hydrocarbons was more stable at room temperature compared to other active functional groups.

Peakfit software was used to perform peak fitting on the infrared spectra in the wavenumber ranges of 3600–3700, 3000–3600, 2800–3000, and 1300–1800 cm^{−1}.^{32–34} The peak fitting curve for the non-water-immersed long-flame coal is shown in Figure 9, with the same method applied to the peak fitting analysis of the other experimental coal samples.

Figure 9a shows that in the range of 1300–1800 cm^{−1}, V₁ corresponds to the vibration of the carbon–carbon double bond (C=C), V₂ corresponds to the vibration of the carbonyl group (C=O), and V₃ corresponds to the vibration of the carboxyl group (–COOH). Figure 9b shows that in the range of 2800–3000 cm^{−1}, V₄ and V₅ correspond to symmetric and antisymmetric stretching vibrations of saturated C–H bonds (CH₃ and CH₂), respectively. Figure 9c shows the wide peak characteristics of hydroxyl (–OH) corresponding to V₆ in the range 3000–3600 cm^{−1}. Figure 9d shows the vibration of V₇ corresponding to the free hydroxyl group (–OH) in the range of 3600–3700 cm^{−1}.

Figure 10 shows the percentage of aliphatic hydrocarbons, aromatic hydrocarbons, oxygen-containing functional groups,

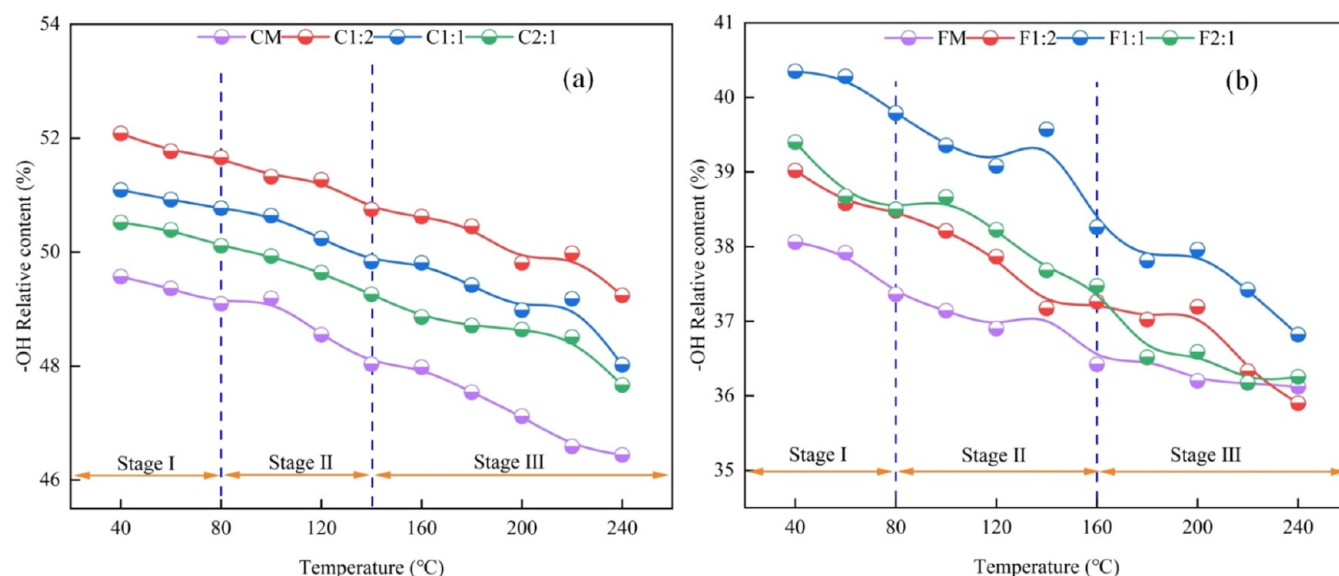


Figure 11. Changes of percentage of hydroxyl content in coal with temperature under different water leaching conditions: (a) long-flame coal; (b) fat coal.

and hydroxyl groups in long-flame coal and aliphatic coal under different water leaching conditions at 40 °C.

As illustrated in Figure 10, the content of hydroxyl groups (–OH) in coal increases notably at 40 °C with even a slight amount of water immersion. Specifically, the hydroxyl contents for C1:2 and F1:1 are the highest, at 52.08 and 40.35%, respectively. This can be attributed to the fact that following water immersion, coal surfaces and internal pores absorb moisture. The hydrogen–oxygen (H–O–H) bonds in water molecules interact with active sites on the coal surface, such as free radicals or unsaturated bonds, leading to the formation of hydroxyl groups.³⁵ When the mass ratio of water to long-flame coal is 1:2, and that of water to fat coal is 1:1, hydroxyl oxidation generates more carbonyl groups (C=O) and carboxyl groups (–COOH), the percentage of which increases from 1.48, 8.35, 5.6, and 9.00% of raw coal to 1.91, 8.91, 6.28, and 9.58%, respectively. At this stage, the rise in hydroxyl groups further triggers a chain reaction involving aliphatic hydrocarbons (–CH₃/–CH₂), resulting in the consumption of more of these groups and consequently a reduction in their percentage content. This reduces from the original coal's 26.41 and 18.19% to 23.14 and 15.59%, respectively. Due to the relatively stable molecular structure of aromatic hydrocarbons, they are less likely to participate in reactions during the low-temperature oxidation process. Consequently, their content experiences only minor fluctuations.³⁶

Moreover, the optimal levels of water immersion that correspond to the highest self-ignition tendencies differ significantly between long-flame coal and fat coal. Because of its lower metamorphic grade, long-flame coal possesses a greater number of pore fractures, resulting in a higher proportion of macro- and mesopores compared to other coal types. As a result, when the water-to-coal mass ratio is 1:2, water is able to penetrate the pores more effectively and make thorough contact with the active sites, thereby greatly enhancing the oxidation reactions within the coal. Fat coal, having undergone a higher degree of metamorphism, possesses a more compact pore structure characterized by a greater proportion of smaller pores. At a water-to-coal mass ratio of 1:1, water is able to more efficiently infiltrate the pores, thereby enhancing the activation

of surface active sites in fat coal. However, when bituminous coal is soaked in excess water, the hydroxyl (–OH) groups in the water preferentially bond with hydrogen bonds in the coal structure, resulting in a decrease in the hydroxyl content in the coal, which in turn leads to a decrease in the carbonyl and carboxyl content.^{3,13} At the same time, the content of aromatic hydrocarbons (C=C) increases, which reduces the oxidation activity of coal.

3.3.2. Examination of How Water Immersion Affects the Staged Evolution of Active Functional Groups in Coal. Under different water immersion conditions, Figures 11–14 illustrate the variation in the percentage content of aliphatic and aromatic hydrocarbons, oxygen-containing functional groups, and hydroxyl groups in both long-flame and fat coal as the temperature rises from 40 to 240 °C.

Figure 11 demonstrates that under various water immersion conditions, the percentage of hydroxyl groups (–OH) in both long-flame coal and fat coal initially decreases gradually, followed by a more rapid decline as the temperature rises. Additionally, the relative content of –OH in coal samples that have undergone water immersion is greater than that in the original, nonimmersed coal. In the early stage of temperature-induced oxidation, the reduction in the percentage of hydroxyl groups (–OH) in both untreated and water-immersed coal occurs gradually. As the moisture adsorbed on the coal's surface evaporates, hydroxyl groups are mainly consumed through mild chemical reactions with oxygen. In this phase, the reaction temperature remains relatively low, leading to a slow rate of –OH consumption, which is reflected in a gradual decrease over time. Additionally, water immersion postpones the rise in the reaction temperature of the coal sample, resulting in a slower rate of hydroxyl group consumption in the water-immersed coal compared to the untreated samples.

During the second stage of temperature-driven oxidation, the oxidation rate of the hydroxyl groups in the untreated coal rises sharply. This phase is characterized by the formation of coal-oxygen complexes, leading to the generation of carbonyl groups (C=O). These carbonyl groups then participate in further reactions, leading to the formation of carboxyl groups (–COOH) and other oxygen-containing functional groups.

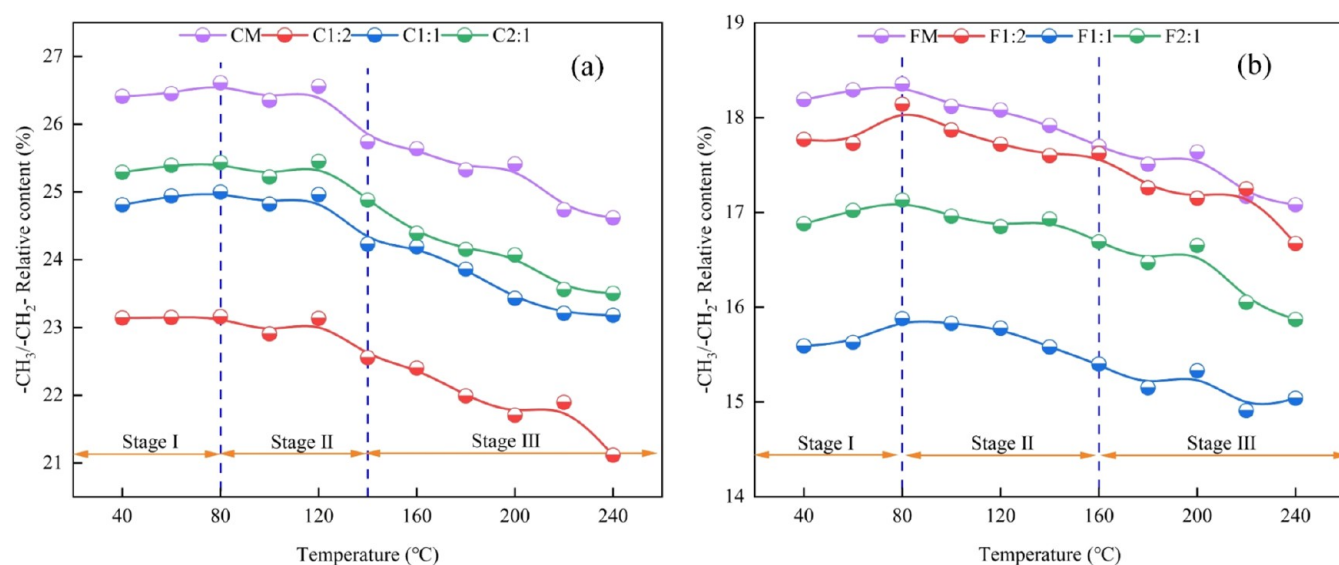


Figure 12. Changes of the percentage of aliphatic hydrocarbon content of long-flame coal and fat coal with temperature under different water leaching conditions: (a) long-flame coal; (b) fat coal.

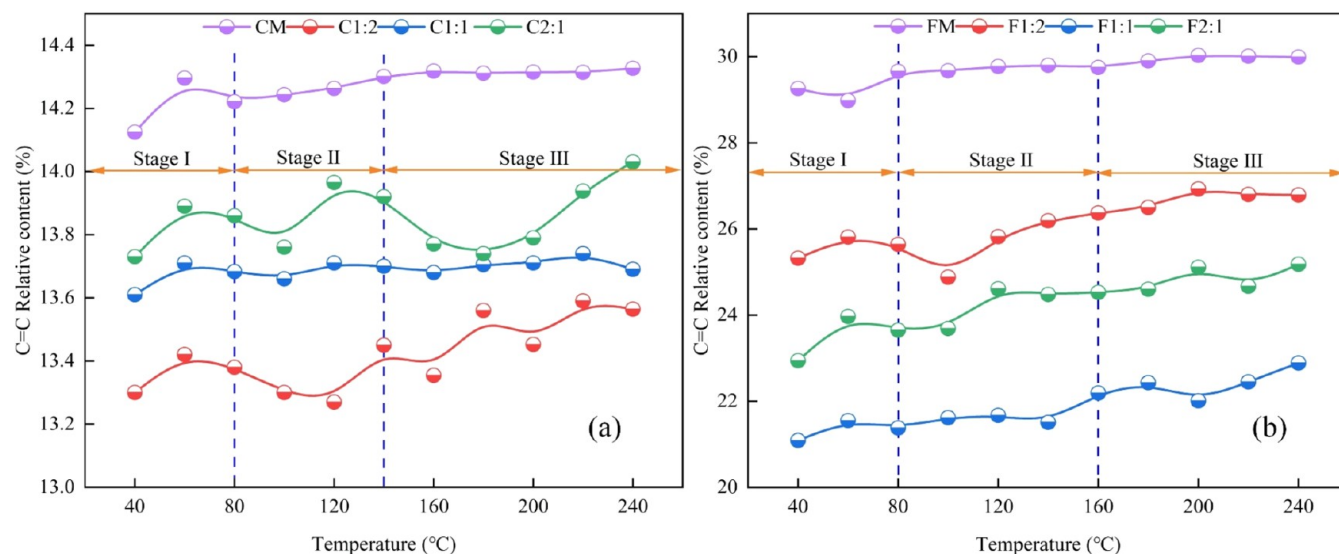


Figure 13. Change of percentage of aromatic hydrocarbon content of long-flame coal and fat coal with temperature under different water leaching conditions: (a) long-flame coal; (b) fat coal.

Simultaneously, as the active sites within the coal structure are activated, the diffusion and reactivity of oxygen are significantly improved, leading to faster depletion of hydroxyl groups. This is reflected in a sharp decrease in the trend. Following water immersion, the coal structure experiences an increase in pore fissures, which enhances the rate of oxygen diffusion. Consequently, the reaction rate of $-\text{OH}$ groups in the water-immersed coal samples is significantly higher compared with the untreated coal, leading to a faster reduction in the hydroxyl group content. In the third stage of temperature-induced oxidation, following water immersion, the increased number of hydroxyl groups further enhances their involvement in oxidation processes, leading to their transformation into carbonyl and carboxyl groups or their direct participation in carbon–oxygen chain reactions. Because of the heightened reaction intensity during this stage, the rate at which hydroxyl groups are consumed peaks, reaching its highest point.

Figure 12 illustrates that under various water immersion conditions, the behavior of aliphatic hydrocarbons ($-\text{CH}_3/-\text{CH}_2-$) in the oxidation process of both long-flame and fat coal begins with a gradual increase, which is then followed by a rapid decline. Moreover, water immersion leads to a reduction in the concentration of aliphatic hydrocarbons in the untreated coal. During the slow oxidation phase, the oxidation of coal is mainly governed by physical adsorption and weak chemical interactions, resulting in limited breakdown or transformation of the aliphatic hydrocarbon groups. As the consumption of aliphatic hydrocarbons is relatively low, their proportion within the functional groups gradually rises. The presence of a surface water film on water-immersed coal samples reduces the oxygen diffusion rate, hindering the reactions and leading to a slower change in their content.

In the rapid oxidation phase, as the temperature increases, the activity of the aliphatic hydrocarbon groups significantly intensifies, leading to chain scission reactions. This process

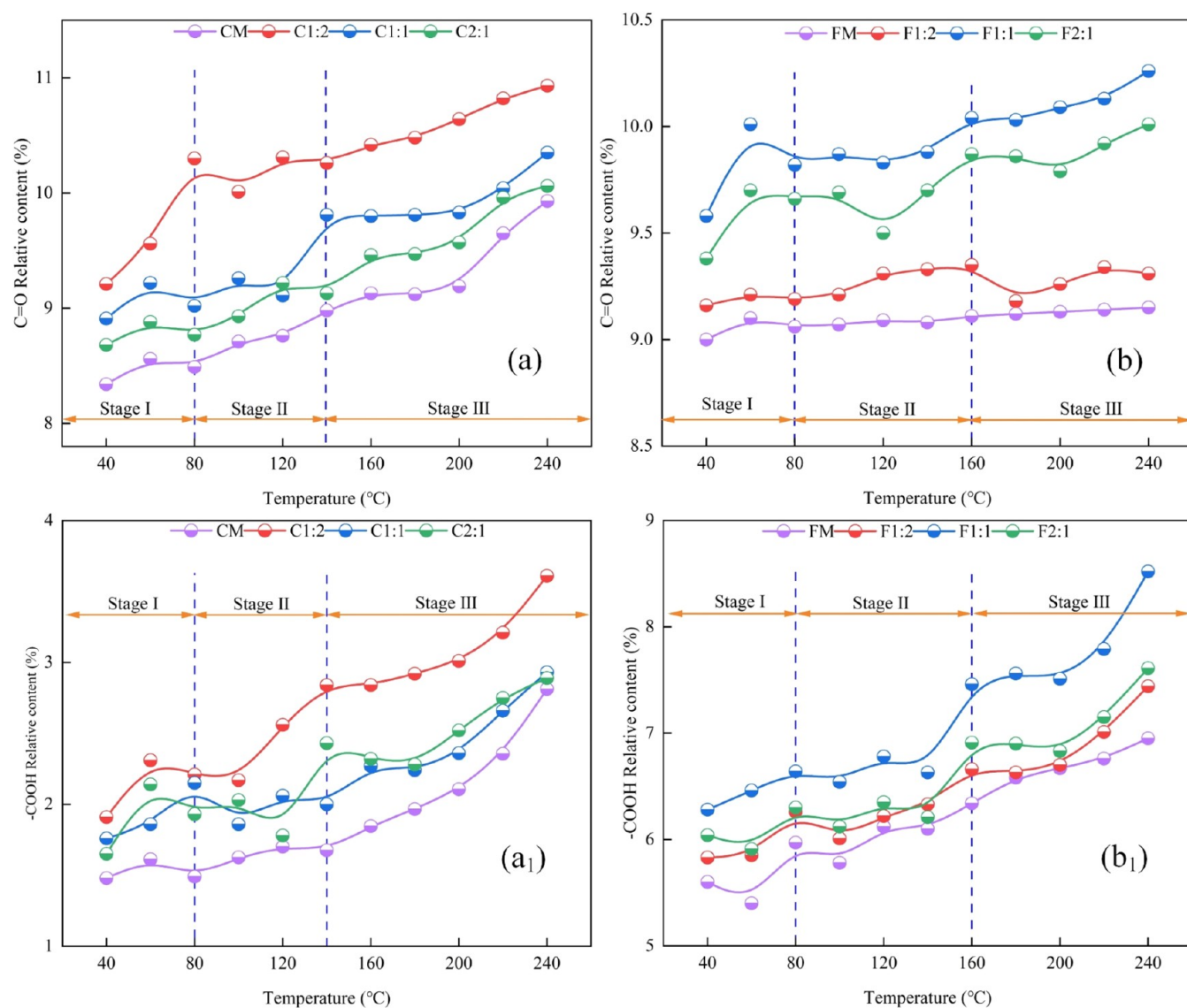


Figure 14. Changes of oxygen-containing functional group content percentage of long-flame coal and fat coal with temperature under different water leaching conditions: (a, a₁) long-flame coal; (b, b₁) fat coal.

generates a considerable amount of radicals, including $-\text{CH}_3$ and $-\text{CH}_2$. At this stage, the free radicals undergo further reactions with oxygen, leading to the formation of peroxide or alcohol intermediates, accompanied by the release of heat. In water-soaked coal, the more developed pore structure facilitates faster oxygen diffusion, which accelerates the oxidation of the aliphatic hydrocarbons. As a result, the content of these hydrocarbons decreases more significantly compared with untreated coal. In the intense oxidation stage, the chain scission of the aliphatic hydrocarbon groups becomes more pronounced. The free radicals produced primarily transform into gaseous byproducts like CO and CO_2 , resulting in the release of significant heat. At this stage, the rate of consumption of aliphatic hydrocarbons peaks, causing their content to decrease rapidly. The increased porosity and enhanced oxygen availability in water-soaked coal samples lead to more vigorous reactions of aliphatic hydrocarbon groups. As a result, a larger number of free radicals are generated, which further accelerates the intense combustion reactions of bituminous coal.

As depicted in Figure 13, the proportion of the $\text{C}=\text{C}$ content steadily increases with the rise in oxidation temperature,

although the rate of this increase remains relatively gradual. This can be explained by the fact that aromatic hydrocarbons exhibit limited reactivity during the oxidation process at temperatures below 220 °C, due to their relatively stable molecular structure. The proportion of aromatic rings increases slightly during oxidation, likely due to the cleavage of the side chains attached to them. Following water immersion treatment, the relative content of aromatic rings in both long-flame coal and fat coal decreases. This suggests that water immersion alters the concentration of other active groups, thereby influencing the proportion of aromatic hydrocarbons and, consequently, impacting the entire temperature oxidation process.

Figure 14 illustrates that the levels of carbonyl ($\text{C}=\text{O}$) and carboxyl (COOH) groups consistently increase in both untreated and water-immersed coal samples during the heating and oxidation phases. During the initial phase of slow oxidation, the reduced reaction temperature between coal and oxygen slows the oxidation of $-\text{OH}$ and $-\text{CH}_3/-\text{CH}_2$ groups, leading to the gradual accumulation of carbonyl and carboxyl groups. Moreover, immersing the coal in water decreases the interaction surface between oxygen and the coal, which in turn slows the

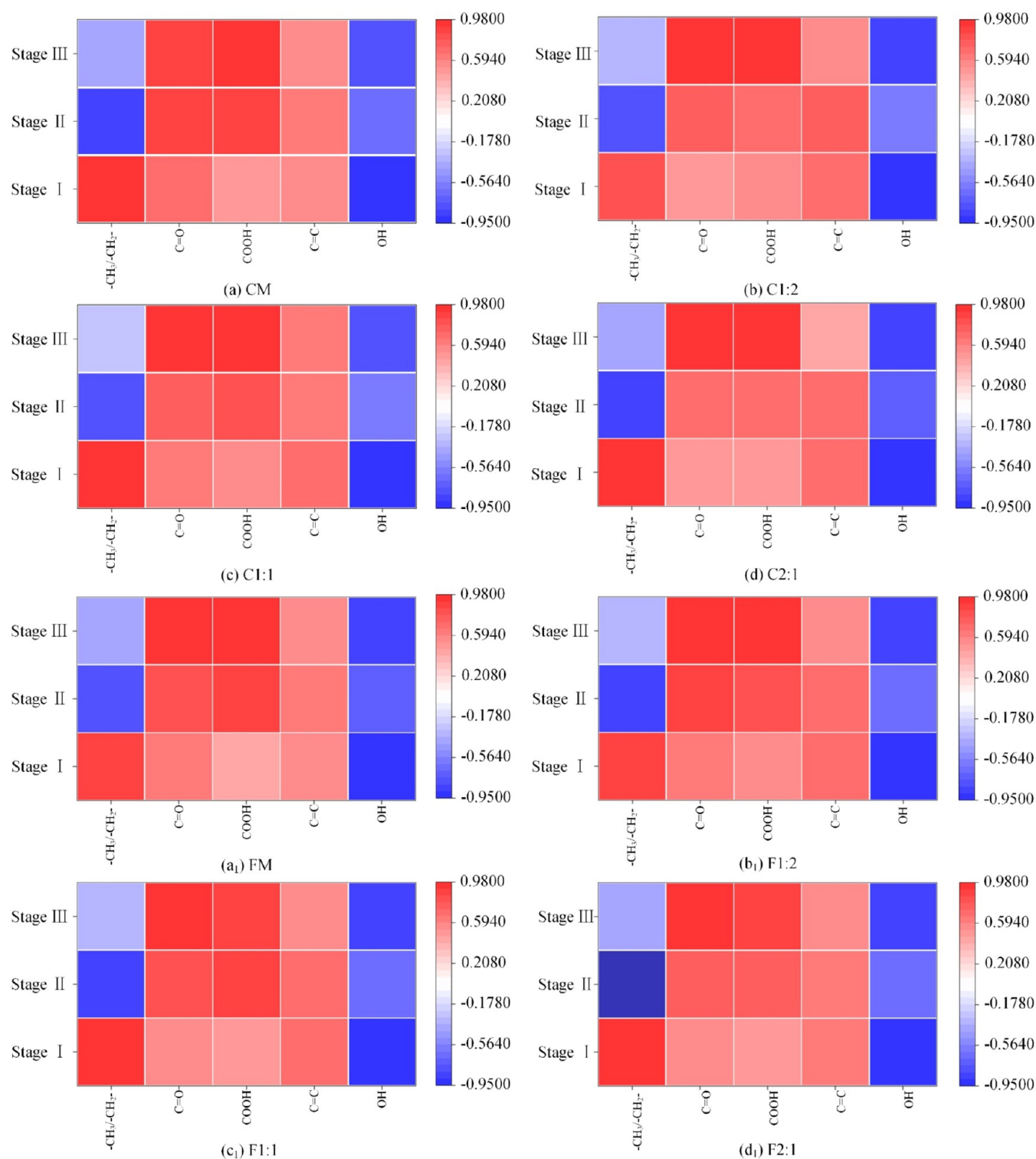


Figure 15. Correlation coefficients of active groups in bituminous coal: (a–d) long-flame coal and (a₁–d₁) fat coal under different water leaching conditions and each temperature rise oxidation stage.

formation rate of C=O and COOH groups in the water-soaked samples relative to the untreated coal.

During the rapid oxidation phase, the rate at which carbonyl and carboxyl groups form rises significantly. As the temperature increases, the aliphatic and aromatic side chains break down more quickly, reacting with oxygen to produce considerable amounts of C=O and –COOH functional groups. Simultaneously, the oxidation of hydroxyl groups intensifies, leading to

the generation of additional precursor groups that facilitate the formation of carbonyl and carboxyl groups. In water-immersed coal samples, the enhanced pore structure and improved oxygen diffusion capacity facilitate the increased formation of C=O and –COOH groups. The rates at which carbonyl and carboxyl groups form peak during the intense oxidation phase. In this phase, the oxidation reactions are primarily driven by decomposition and intense oxidation, resulting in the formation

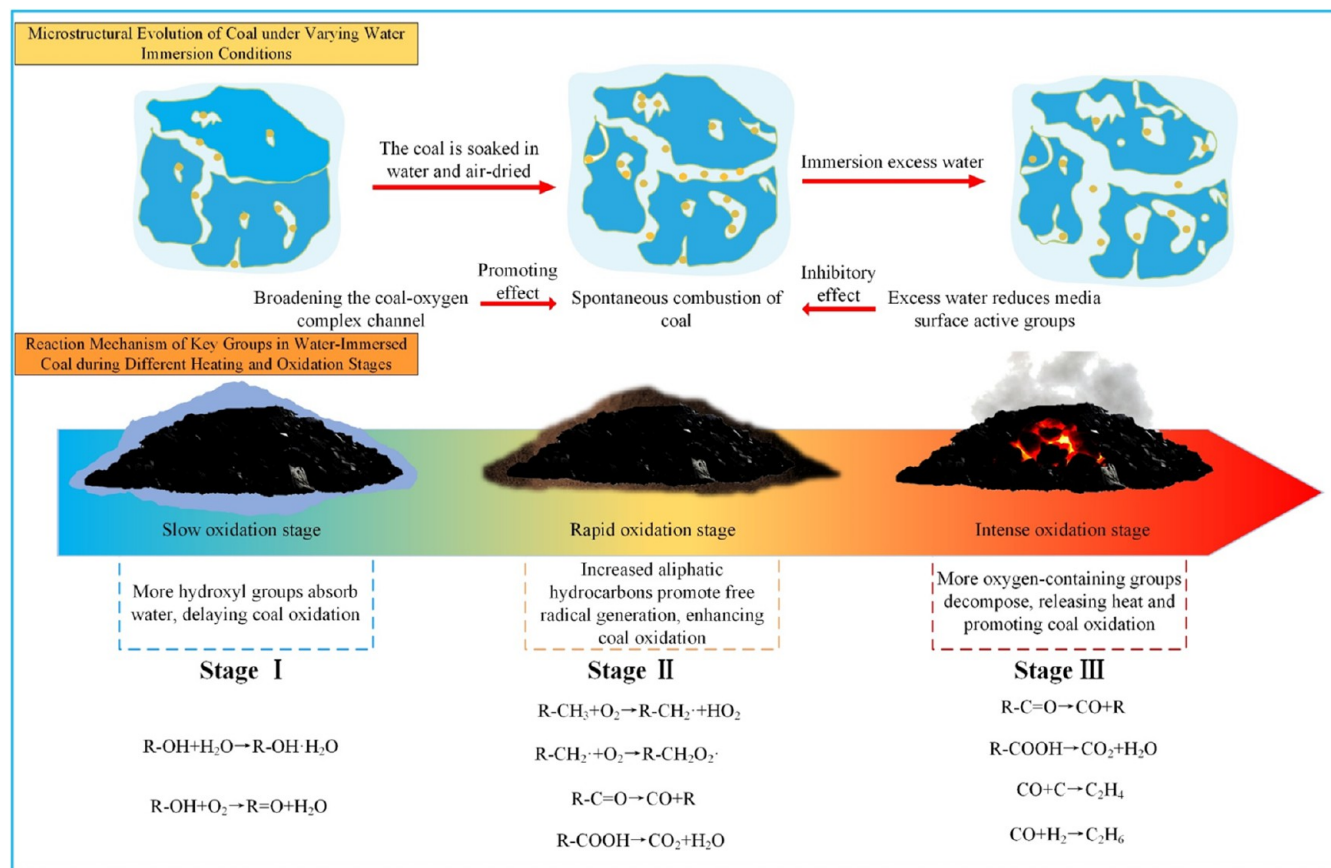


Figure 16. Spontaneous combustion tendency and microstructure change mechanism of the immersed coal sample in the heating oxidation stage.

of a large quantity of C=O and -COOH functional groups. These groups undergo further oxidation, leading to the production of small molecular products like CO, CO₂, and water, accompanied by the release of substantial heat. The oxidation of aliphatic hydrocarbons and aromatic ring side chains persists, supplying precursors for the formation of C=O and -COOH groups. In the case of the water-immersed coal sample, which has a greater number of active sites, the decomposition and oxidation reactions are more pronounced. This leads to a sustained high level of C=O and -COOH contents throughout the high-temperature stage.

3.3.3. Analysis of the Correlation between Functional Groups and Coal Heating and Oxidation Stages. This study utilizes Pearson correlation analysis to investigate the key reactive groups present in long-flame coal and fat coal under varying water immersion conditions across different stages of heating and oxidation. Figure 15 shows the correlation coefficients between the functional groups in both untreated and water-immersed coal samples at various stages of heating and oxidation.

Figure 15 indicates that while water immersion treatment did not alter the overall correlation pattern between the experimental coal samples and their functional groups at each heating and oxidation stage, there were variations in the correlation coefficients. In the initial (slow oxidation) stage, the hydroxyl group (-OH) shows the strongest correlation with both fat coal and long-flame coal. For non-water-treated long-flame coal and fat coal, the correlation coefficients are -0.955 and -0.941, respectively. This suggests that the hydroxyl group plays a crucial role during this stage. Due to its strong polarity,

the hydroxyl group is capable of adsorbing water, forming a water layer that covers the coal surface. This water coverage effectively occupies the active sites, limiting the interaction between oxygen and the coal, which, in turn, slows down the oxidation process. This reduces the interaction between oxygen and coal, thereby slowing the oxidation reaction. The analysis reveals that water immersion treatment notably enhanced the proportion of hydroxyl groups in both fat coal and long-flame coal. The presence of moisture further infiltrates the coal's pore structure, effectively isolating oxygen and thereby decreasing the likelihood of spontaneous combustion during this phase.

During the second stage, which is the rapid oxidation phase, the correlation coefficients between fat coal, long-flame coal, and aliphatic hydrocarbons (-CH₃/-CH₂-) are the highest, reaching -0.876 and -0.892, respectively. This suggests that aliphatic hydrocarbons play a crucial role in this phase. During this stage, the aliphatic hydrocarbon chains undergo cleavage, producing a substantial number of free radicals such as -CH₃, and releasing considerable heat. This process significantly accelerates the coal's oxidation reaction. The free radicals produced may also interact with other functional groups, leading to the formation of intermediate compounds, such as peroxides or alcohols. This process further generates heat, thereby increasing the likelihood of spontaneous combustion. The findings reveal that water immersion notably raised the proportion of aliphatic hydrocarbons in both fat coal and long-flame coal, thereby supplying a greater amount of reactants for the oxidation process and increasing the coal's reactivity.

In the third stage (intense oxidation stage), the spontaneous combustion process of bituminous coal has the highest

correlation with oxygen-containing functional groups. The correlation coefficients of fat coal and long-flame coal with a carbonyl group ($\text{C}=\text{O}$) are 0.934 and 0.980, and the correlation coefficients with a carboxyl group ($-\text{COOH}$) are 0.859 and 0.913, respectively. This shows that the oxygen-containing functional group is the key group in this stage. This indicates that in this phase oxygen-containing functional groups are pivotal in the oxidation process. At higher temperatures, functional groups such as carbonyl and carboxyl undergo swift decomposition, leading to the release of large quantities of CO_2 , H_2O , and a smaller amount of CO , while also generating considerable heat. This increases the coal's propensity for vigorous combustion reactions. Water immersion treatment increases the concentration of oxygen-containing functional groups in both fat coal and long-flame coal, thereby supplying more reactants for the oxidation process at higher temperatures. As a result, the oxidation reaction within the coal becomes more intense. Additionally, the CO and CO_2 produced during the breakdown of oxygen-containing groups can undergo further oxidation or secondary reactions. This leads to the generation of flammable gases, such as ethylene and ethane, which accelerates the spontaneous combustion of the coal.

3.3.4. Investigation into the Mechanism of Water Immersion Treatment during the Low-Temperature Oxidation Stages of Bituminous Coal. This research explores how water immersion affects bituminous coal at various heating and oxidation stages, revealing the underlying mechanisms and trends of its impact, as depicted in Figure 16.

As depicted in Figure 16, even a small amount of water immersion results in the development of a more complex coal-oxygen interaction pathway within the coal's internal pore structure. This facilitates better oxygen adsorption and diffusion at lower temperatures, thereby increasing the number of active sites available on the coal's surface. Consequently, the rate of spontaneous combustion in coal is significantly enhanced. However, when water immersion exceeds a certain level, the coal's pore structure becomes fully saturated, which hinders the diffusion of oxygen. As a result, the number of active functional groups on the coal surface decreases, leading to a decrease in the rate of low-temperature oxidation.

Significant differences are observed in the spontaneous combustion behaviors and primary reaction mechanisms of the coal samples with water immersion across the three heating and oxidation stages. In the slow oxidation stage, the hydroxyl ($-\text{OH}$) group acts as a key reactive site. Its tendency to absorb water results in the formation of a water layer on the coal surface, which subsequently restricts direct contact between oxygen and the coal. This notably delays the initiation of the oxidation reaction. As the process advances into a rapid oxidation stage, aliphatic hydrocarbons ($-\text{CH}_3/-\text{CH}_2-$) become the dominant reactive groups. During the chain scission process, aliphatic hydrocarbons break down to form a large number of free radicals (such as $-\text{CH}_3$), along with small amounts of CO and CO_2 , and the release of significant heat. This combination of factors accelerates the coal's oxidation reaction. As the process advances into the rapid oxidation phase, oxygen-containing functional groups such as carbonyl ($\text{C}=\text{O}$) and carboxyl ($-\text{COOH}$) undergo intense decomposition. This reaction produces CO_2 , H_2O , and CO , releasing significant heat in the process. This greatly speeds up the coal oxidation process. Moreover, the CO and CO_2 generated during the decomposition reactions can engage in secondary reactions, producing flammable gases such

as ethylene and ethane. This, in turn, intensifies the spontaneous combustion tendency of the coal.

4. CONCLUSIONS

In this study, scanning electron microscopy, low-temperature nitrogen adsorption experiment, in situ Fourier transform infrared spectroscopy experiment, Pearson correlation analysis, and other methods were used. It investigated the variation patterns of coal pore and fracture structures, spontaneous combustion characteristics, and the correlation between key functional groups and heating oxidation stages for long-flame coal and fat coal under three different water immersion conditions. The comprehensive analysis leads to the following conclusions:

- (1) As water immersion increases, both the number and average size of pores and fractures in bituminous coal steadily increase. The water molecules cause the coal samples to swell and fracture, leading to a greater proportion of mesopores and macropores in the water-immersed coal. When the mass ratio of water to long-flame coal and fat coal reaches 2:1, the peak values are 21.87, 19.64% and 78.16, 73.24%, respectively. As a result, the contact area between the coal and oxygen is significantly enhanced, making the water-immersed coal more susceptible to spontaneous combustion.
- (2) The impact of water immersion on the spontaneous combustion behavior of bituminous coal differs across various stages of heating and oxidation. In the slow oxidation phase, water immersion raises the moisture level within the coal's internal pores, thereby delaying the onset of the oxidation reaction in the coal sample. At this stage, the oxygen consumption rate is highest for both long-flame coal and fat coal prior to water immersion. Their oxygen concentrations decrease from 20.52 and 20.44% to 18.61 and 18.02%, respectively. In the rapid oxidation and intense oxidation stages, water immersion causes the coal's internal structure to become looser, increasing the pore area and enhancing its capacity to absorb oxygen. This makes the coal more prone to spontaneous combustion. At 220 °C, the CO production for C1:2 and F1:1 reaches its peak, with concentrations of 23,157 and 25,699 ppm, respectively. This represents a 1.83- and 1.48-fold increase compared to untreated coal.
- (3) In the rapid and intense oxidation stages, the spontaneous combustion propensity of both long-flame coal and fat coal increases with the initial rise in water immersion. However, as the level of immersion continues to increase, this tendency starts to decline. When the mass ratio of water to long-flame coal is 1:2, and the mass ratio of water to fat coal is 1:1, the tendency for spontaneous combustion is highest. At this time, C1:2 and F1:1 in the intense oxidation stage (stage III) have the lowest activation energy of 8.4 and 18.74 kJ/mol, respectively, which represents a reduction of 21.2 and 33.5% compared to raw coal. As the amount of water immersion increases further, the activation energy of the coal sample also increases, leading to a reduction in its tendency for spontaneous combustion. At this point, water immersion exerts an inhibitory effect on the coal, reversing its earlier impact.
- (4) The water immersion treatment did not alter the overall correlation pattern between the experimental coal

samples and their functional groups at each heating and oxidation stage; instead, only variations in the correlation coefficients were observed. During the slow oxidation stage, the $-OH$ group serves as the primary functional group in both long-flame coal and fat coal, exhibiting correlation coefficients of -0.955 and -0.941 , respectively. In the rapid oxidation stage, aliphatic hydrocarbons are the dominant reactive groups, with correlation coefficients of -0.876 for long-flame coal and -0.892 for fat coal. In the intense oxidation stage, oxygen-containing functional groups ($C=O$, $-COOH$) become the key functional groups for both long-flame coal and fat coal, showing correlation coefficients of 0.934 and 0.980 for long-flame coal, and 0.859 and 0.913 for fat coal.

AUTHOR INFORMATION

Corresponding Author

Jiuyuan Fan – School of Emergency Management and Safety Engineering, North China University of Technology, Tangshan 063210, P. R. China; Key Laboratory of Mining Development and Safety Technology, Tangshan 063210, P. R. China; orcid.org/0009-0008-1017-6006; Phone: +8613273543090; Email: fanjiuyuan@ncst.edu.cn

Authors

Jiangtao Li – School of Emergency Management and Safety Engineering, North China University of Technology, Tangshan 063210, P. R. China; Key Laboratory of Mining Development and Safety Technology, Tangshan 063210, P. R. China; orcid.org/0009-0003-2807-3455

Chuyan Sun – School of Emergency Management and Safety Engineering, North China University of Technology, Tangshan 063210, P. R. China; Key Laboratory of Mining Development and Safety Technology, Tangshan 063210, P. R. China

Jiuling Zhang – School of Emergency Management and Safety Engineering, North China University of Technology, Tangshan 063210, P. R. China; Key Laboratory of Mining Development and Safety Technology, Tangshan 063210, P. R. China

Shuliang Xie – College of Safety and Environment Engineering, Shandong University of Science and Technology, Qingdao 266590, P. R. China; orcid.org/0009-0000-8705-0163

Dong Gao – School of Emergency Management and Safety Engineering, North China University of Technology, Tangshan 063210, P. R. China; Key Laboratory of Mining Development and Safety Technology, Tangshan 063210, P. R. China

Complete contact information is available at:

<https://pubs.acs.org/10.1021/acsomega.4c10912>

Notes

The authors declare no competing financial interest.

ACKNOWLEDGMENTS

This study was sponsored by the Natural Science Foundation of Hebei Province (E2022209101) and the National Natural Science Foundation of China (51504077 and 51404086).

REFERENCES

- (1) Liu, H.; Li, Z.; Yang, Y.; et al. Role of moisture content in coal oxidation during the spontaneous combustion latency. *Energy* **2024**, *291*, No. 130336.
- (2) Li, T.; Zhao, H.; Qi, Y.; et al. Study on preparation and properties of steel slag based composite gel for mine fire prevention and extinguishing. *Arab. J. Chem.* **2024**, *17* (10), No. 105966.
- (3) Fan, J.; Li, J.; Zhang, J.; et al. Study on Spontaneous Combustion Characteristics and Microstructure of Bituminous Coal under Water Immersion. *ACS Omega* **2024**, *9* (33), 35950–35960.
- (4) Yuan, J.; Lei, Q.; Xiong, M.; et al. The prospective of coal power in China: Will it reach a plateau in the coming decade? *Energy Policy* **2016**, *98*, 495–504.
- (5) Niu, H.; Liu, Y.; Wu, K.; et al. Study on pore structure change characteristics of water-immersed and air-dried coal based on SEM-BET. *Combust. Sci. Technol.* **2023**, *195* (16), 3994–4016.
- (6) Zhai, X.; Song, B.; Wang, B.; et al. Study on the effect and mechanism of water immersion on the characteristic temperature during coal low-temperature oxidation. *Nat. Resour. Res.* **2021**, *30*, 2333–2345.
- (7) Bu, Y.-c.; Niu, H.; Wang, H.; et al. Characteristics of lean oxygen combustion and dynamic microreaction process of water-soaked coal. *Fuel* **2023**, *332*, No. 126010.
- (8) Bu, Y.-c.; Niu, H.; Qiu, T.; et al. Analysis of stage parameters of low-temperature oxidation of water-soaked coal based on kinetic principles. *Sci. Total Environ.* **2024**, *946*, No. 173947.
- (9) Zhang, X.; Liang, H.; Lu, B.; et al. Stage changes in the oxidizing properties of long-term water-soaked coal and analysis of key reactive groups. *Fuel* **2024**, *358*, No. 130186.
- (10) Zhang, L.; Wen, C.; Li, S.; Yang, M. Evolution and oxidation properties of the functional groups of coals after water immersion and air drying. *Energy* **2024**, *288*, No. 129709.
- (11) Deng, J.; Qu, G.; Ren, S.; et al. Effect of water soaking and air drying on the thermal effect and heat transfer characteristics of coal oxidation at the low-temperature oxidation stage. *Energy* **2024**, *288*, No. 129705.
- (12) Liu, Q.; Sun, L.; Zhang, Y.; et al. Effects of water immersion and pre-oxidation on re-ignition characteristics of non-caking coal. *Energy* **2023**, *282*, No. 128616.
- (13) Huang, Z.; Li, J.; Gao, Y.; et al. Thermal behavior and microscopic characteristics of water-soaked coal spontaneous combustion. *Combust. Sci. Technol.* **2022**, *194* (3), 636–654.
- (14) Zhang, X.; Li, C.; Lu, B.; et al. Effect of high geothermal environments on microscopic properties and oxidation processes of waterlogged coal. *Case Stud. Therm. Eng.* **2024**, *64*, No. 105496.
- (15) Zhong, X.; Kan, L.; Xin, H.; et al. Thermal effects and active group differentiation of low-rank coal during low-temperature oxidation under vacuum drying after water immersion. *Fuel* **2019**, *236*, 1204–1212.
- (16) Guo, S.; Geng, W.; Yuan, S.; et al. Kinetic analysis of coal oxidative pyrolysis before and after immersion effect. *Case Stud. Therm. Eng.* **2024**, *63*, No. 105235.
- (17) Lu, W.; Li, J.; Li, J.; et al. Oxidative kinetic characteristics of dried soaked coal and its related spontaneous combustion mechanism. *Fuel* **2021**, *305*, No. 121626.
- (18) Huang, Z.; Tian, Y.; Gao, Y.; et al. Study on the oxidation kinetics and microactivity of water-immersed coal. *ACS Omega* **2020**, *5* (28), 17287–17303.
- (19) Zhai, X.; Ge, H.; Wang, T.; et al. Effect of water immersion on active functional groups and characteristic temperatures of bituminous coal. *Energy* **2020**, *205*, No. 118076.
- (20) Liu, H.; Li, Z.; Yang, Y.; et al. Investigation of the effect of different distilled water, rainwater and seawater mass ratios on coal spontaneous combustion characteristics. *Sci. Total Environ.* **2023**, *900*, No. 165878.
- (21) Fan, J.; Wang, G.; Zhang, J. Study on spontaneous combustion tendency of coals with different metamorphic grade at low moisture content based on TPO-DSC. *Energies* **2019**, *12* (20), 3890.
- (22) Jiang, L.; Sheng, C. Correlation of the sub-micrometer ash yield from pulverized coal combustion with coal ash composition. *Energy Fuels* **2018**, *32* (9), 9961–9970.
- (23) Luo, Z.; Qin, B.; Shi, Q.; et al. Compound effects of water immersion and pyritic sulfur on the microstructure and spontaneous combustion of non-caking coal. *Fuel* **2022**, *308*, No. 121999.
- (24) Song, Y.; Yang, S.; Xu, Q.; et al. Effect of low-temperature oxidation of coal with different metamorphic degrees on coal quality

characteristics and outburst comprehensive index. *Process Saf. Environ. Prot.* **2019**, *132*, 142–152.

(25) Wang, H.; Dlugogorski, B. Z.; Kennedy, E. M. Role of inherent water in low-temperature oxidation of coal. *Combust. Sci. Technol.* **2003**, *175* (2), 253–270.

(26) He, Y. J.; Deng, J.; Zhai, X. W.; et al. Experimental investigation of the macroscopic characteristic parameters and microstructure of water-soaked coal during low-temperature oxidation. *J. Therm. Anal. Calorim.* **2022**, *147* (17), 9711–9723.

(27) Zhou, B.; Yang, S.; Jiang, X.; et al. The reaction of free radicals and functional groups during coal oxidation at low temperature under different oxygen concentrations. *Process Saf. Environ. Prot.* **2021**, *150*, 148–156.

(28) Chen, S.; Tao, S.; Tang, D.; et al. Pore structure characterization of different rank coals using N₂ and CO₂ adsorption and its effect on CH₄ adsorption capacity: A case in Panguan syncline, western Guizhou, China. *Energy Fuels* **2017**, *31* (6), 6034–6044.

(29) Xuanxuan, Z.; Xiufeng, Z.; Qing, G. Classification of spontaneous combustion hazard levels of coal with different metamorphism degrees. *Combust. Sci. Technol.* **2024**, *196* (10), 1459–1472.

(30) Yan, J.; Liu, M.; Feng, Z.; et al. Study on the pyrolysis kinetics of low-medium rank coals with distributed activation energy model. *Fuel* **2020**, *261*, No. 116359.

(31) Zhu, H.; Sheng, K.; Zhang, Y.; et al. The stage analysis and countermeasures of coal spontaneous combustion based on “five stages” division. *PLoS One* **2018**, *13* (8), No. e0202724.

(32) Huang, Z.; Wang, G.; Ding, H.; et al. Study on the inhibition performance of double network physicochemical nanocomposite gel inhibitor on coal spontaneous combustion. *Fuel* **2023**, *350*, No. 128697.

(33) Pi, Z.; Li, R.; Guo, W.; et al. Experimental study on the influence of pore structure and group evolution on spontaneous combustion characteristics of coal samples of different sizes during immersion. *ACS Omega* **2023**, *8* (25), 22453–22465.

(34) Xu, Y. L.; Bu, Y. C.; Chen, M. L.; Wang, L. Y. Effect of water-immersion and air-drying period on spontaneous combustion characteristics for long-flame coal. *Combust. Sci. Technol.* **2022**, *194* (5), 882–897.

(35) Yu, J.; Tahmasebi, A.; Han, Y.; et al. A review on water in low rank coals: The existence, interaction with coal structure and effects on coal utilization. *Fuel Process. Technol.* **2013**, *106*, 9–20.

(36) Zhang, Y.; Zhai, F.; Shu, P.; et al. Study on evolution characteristics of thermal contribution functional groups in low temperature oxidation process of bituminous coal. *Fuel* **2023**, *341*, No. 127683.